Time-resolved Spectroelectrochemical Investigation of Organic Mixed Conductors

Priscila Cavassin§*, and Natalie Banerji*

§SCS-Metrohm Award for best oral presentation in Polymers, Colloids & Interfaces

Abstract: Organic mixed ionic and electronic conductors (OMIECs) are an emerging class of materials that have been applied for a wide range of electrochemical applications. Due to the complexity inherent to the ionic-electronic coupling, understanding the underlying mechanisms involved in the OMIEC operation is an exciting and very lively research field. In this work, we highlight the use of time-resolved Vis-NIR spectroelectrochemistry to characterize these materials. We discuss an example, where we show that by combining this tool with spectral decomposition, we are able to understand fundamental aspects of the doping in an OMIEC film. The methods we present here can be generalized and used to characterize any electrochromic material.

Keywords: Conjugated polymers · Electrochemical doping · OMIECs · Spectroelectrochemistry

Priscila Cavassin is a PhD student in Chemistry and Molecular Sciences at the University of Bern. She holds a master's degree in Applied Physics from the University of São Paulo. Her research focuses on the characterization of organic mixed ionic electronic conductors, and she is especially interested in unraveling the fundamental mechanisms behind these materials.

1. Introduction

Materials that conduct both electronic and ionic species are crucial for a wide range of emerging electrochemical devices, from health to energy technologies.[1] Organic mixed ionic electronic conductors (OMIECs) are among this class and have been gathering attention in the past years due to their easy processability, low power operation and high output. Furthermore, they are biocompatible and good ionic to electronic signaling transducers.[1] For these reasons, OMIECs have emerged as a highly promising category of materials, and have been successfully applied in very different fields, such as neuromorphic devices,[2] biosensors,[3] organ-on-a-chip technologies[4] and light-emitting electrochemical cells.[5]

OMIECs generally involve conjugated polymers (CPs) that can uptake large amounts of ions in their bulk volume and still maintain good electronic conductivity due to their conjugated backbone, or CP/polyelectrolyte composites, in which the ionic transport takes place within the polyelectrolyte phase and the electronic one in the CP-rich phase.

Ionic and electronic transports are coupled through electrochemical doping. In this process, electronic charge carriers are introduced into the organic thin film from an electrode. Simultaneously, counterions from an electrolyte permeate the film to ensure charge neutrality. The conductivity of the film is modulated by the density of charge carriers, controlled by the voltage applied between the film and a counter electrode.[6] This process is reversible, stable and controllable, and is the core of applications involving OMIECs.

The field of OMIECs takes advantage of the extensive literature on the electronic transport of conjugated polymers, that have been studied since the discovery of electronic conductivity in polyacetylene in 1977.[7] It also benefits from the knowledge about ionic transport in solid polymer electrolytes studied in batteries.[8] However, the ionic-electronic coupling plays a fundamental role and therefore it is essential to take a holistic approach when describing OMIECs, taking both electronic and ionic transport into account. This increases the complexity of describing the fundamental mechanisms underlying their performance and opens up new research directions that focus on understanding these processes in OMIECs.

Characterizing these materials using *in situ* and in *operando* techniques is key to following the transient processes of ion injection and electronic charge density increase.[9] With non-time-resolved techniques, only steady-state settings can be probed, and the intermediate states and kinetics are not taken into account. Time-resolved Vis-NIR spectroelectrochemistry, for instance, is a technique that allows probing of the absorbance changes of OMIEC films as they are electrochemically doped. Conjugated polymers typically used as OMIECs are electrochromic, *i.e.* they undergo important absorbance changes during electrochemical doping. Therefore, *in situ*, time-resolved spectroelectrochemistry is a great tool to characterize such OMIECs.

In this work, we will show an example of how Vis-NIR spectroelectrochemistry can be used to answer fundamental questions regarding ionic-electronic coupling in CP-based OMIECs. We discuss how the film morphology impacts the ion transport, doping, and build a kinetic model that describes the steps involved in doping.

2. Time-Resolved Vis-NIR Spectroelectrochemistry

In our recently published work, we use poly(3-hexylthiophene-2,5-diyl) (P3HT), a well-characterized CP, to gain knowledge about the kinetics and the intermediate processes of the electrochemical doping in OMIECs.[6] We deposit the P3HT thin films on a transparent, conductive electrode, and immerse our film in an aqueous 0.1 M KPF_6 electrolyte, together with an Ag/

Correspondence: P. Cavassin, E-mail: priscila.cavassin@unibe.ch; Prof. N. Banerji, E-mail: natalie.banerji@unibe.ch
Department of Chemistry, Biochemistry and Pharmaceutical Sciences, University of Bern, Freiestrasse 3, CH-3012, Bern, Switzerland

AgCl *quasi*-reference counter electrode (Fig. 1a). As we apply voltage between the film and the electrode, we measure the Vis-NIR absorbance changes in the film, as shown in Fig. 1b. It can be observed that initially, for positive voltages, the film absorbs at 500 nm. This is the neutral P3HT band. As we apply more negative voltages (oxidative) to the film, this band is depleted and followed by the rise of a band at 800 nm and at higher wavelengths, around 1400 nm. The band at 800 nm is assigned to the singly charged polymer (P3HT+), which is referred to the field as a polaron. The band at 1400 nm is assigned to the doubly charged polymer (P3HT2+), known as the bipolaron.[10]

Because these bands typically overlap, decomposing the spectra is an important step in obtaining information on the individual evolution/kinetics of different species.

2.1 *Spectral Decomposition*

To decompose spectral data into different signatures and concentrations, we use an optimization method known as Multivariate Curve Resolution (MCR).[11] We start from the unprocessed spectral data, which can be varied with voltage or time. We then use pyMCR, an open-source software library written in Python.[11]

Mathematically, the unmixing of the data is described by a data matrix $D \in \mathbb{U}^{m,n}$, where m is the number of independent measurements and n is the number of elements for a single measurement (such as wavelength). $\mathbb{U}$ represents the universal set of numbers. MCR uses an iterative alternating regression to solve the following equation:

$$D = CS^T + \varepsilon \tag{1}$$

Where $C \in \mathbb{U}^{m,p}$ is the concentration of *p* species and $S \in \mathbb{U}^{n,p}$ are the spectral signatures of the *p* species. $\varepsilon \in \mathbb{U}^{m,n}$ is the error, noise matrix. ε also accounts for limitations that are not captured by the method, such as band shifts.

Typically, the implementation of MCR uses an alternating least-squares approach with either ordinary least squares (OLS) or non-negative least squares (NNLS) regressors.

In order to use MCR, one must stipulate how many species are present in the data. Initial spectral or concentration guesses are also helpful to obtain a meaningful decomposition. If two species have the same evolution in time, for instance, then they cannot be separated by the model.

In this work, we use MCR to decompose our data in Fig. 1b into spectral signatures and concentrations (Fig.1c and d). It is interesting to note that in this case, we can decompose the spectra into 4 species: neutral disordered P3HT, neutral ordered P3HT, polarons, and bipolarons. Because CPs are typically semi-crystalline, and the ordered and disordered domains have different
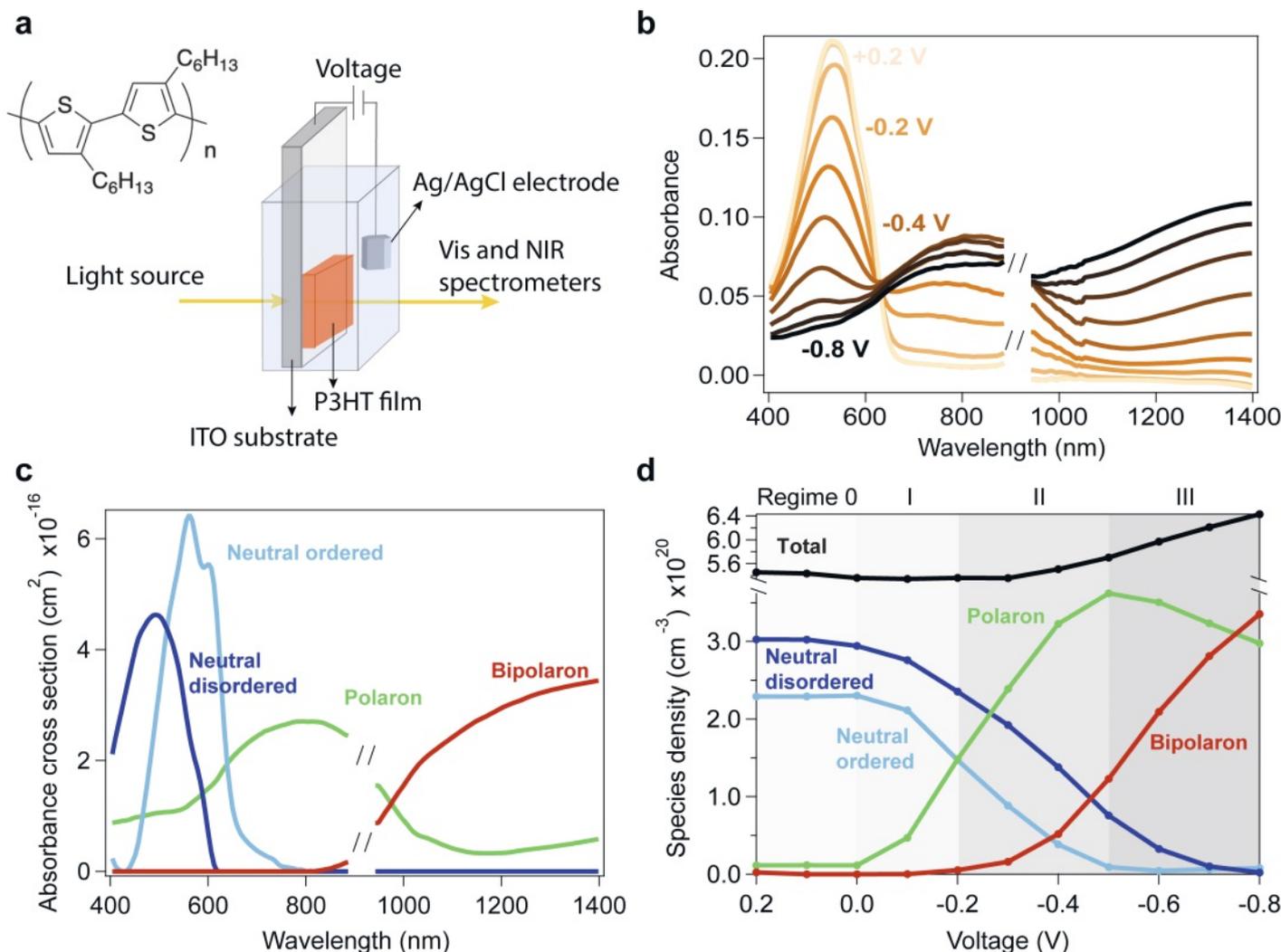
Fig. 1. a) P3HT structure and experiment schematics. b) Absorbance spectra for different doping voltage steps, from 0.2 V to -0.8 V, with steps of -0.1 V. The spectra are decomposed into c) spectral signatures and d) concentrations obtained with the optimization method known as Multivariate Curve Resolution.[6]

absorbance bands, we are able to separate them and evaluate the role of morphology in electrochemical doping.

The concentrations obtained with MCR are not absolute. In order to have meaningful values, we need to determine the absorbance cross section, which is estimated by associating the absorbance to the density of injected charge, measured by chronoamperometry.

The evolution of the concentrations versus voltage shown in Fig. 1d brings interesting information, such as that the ordered domains are doped at lower potentials than the disordered domains, and that initially only polarons are formed (Regime **I**), followed by the formation of bipolarons (Regime **II**) and then by the decrease of polarons that are converted into more bipolarons (Regime **III**).

2.2 Kinetics of the Electrochemical Doping

The doping process in OMIECs is dynamic and evolves with time. For this reason, we now move on to discuss the absorbance changes in time. We apply voltage pulses from a dedoped off-voltage (+0.4 V) to a doped on-voltage varying from -0.1 V to -0.8 V. During each voltage step, the film gets doped (oxidized), and we simultaneously measure the absorbance spectra every 5 ms. We then use MCR decomposition with the same spectral signatures shown in Fig. 1c and obtain the evolution in time for the same four species. Fig. 2 shows the kinetics of doping and dedoping for 3 different voltages, one from each regime defined in the previous section. With the evolution of each species, we are able to build a kinetic model that describes the intermediate steps during the doping and dedoping processes for each regime.

In Regime **I**, polarons are formed within both morphological domains, but they are more numerous in the ordered regions. In Regime **II**, we start to form bipolarons, and they are preferentially formed within the disordered domains, contrary to the singly charged P3HT$^+$. It is only for higher voltages, in Regime **III**, that bipolarons start to form within the more ordered domains. The electrochemical reactions for the doping and dedoping are written next to each panel in Fig. 2, together with the schematic illustration of how the doping is happening within the different mor-
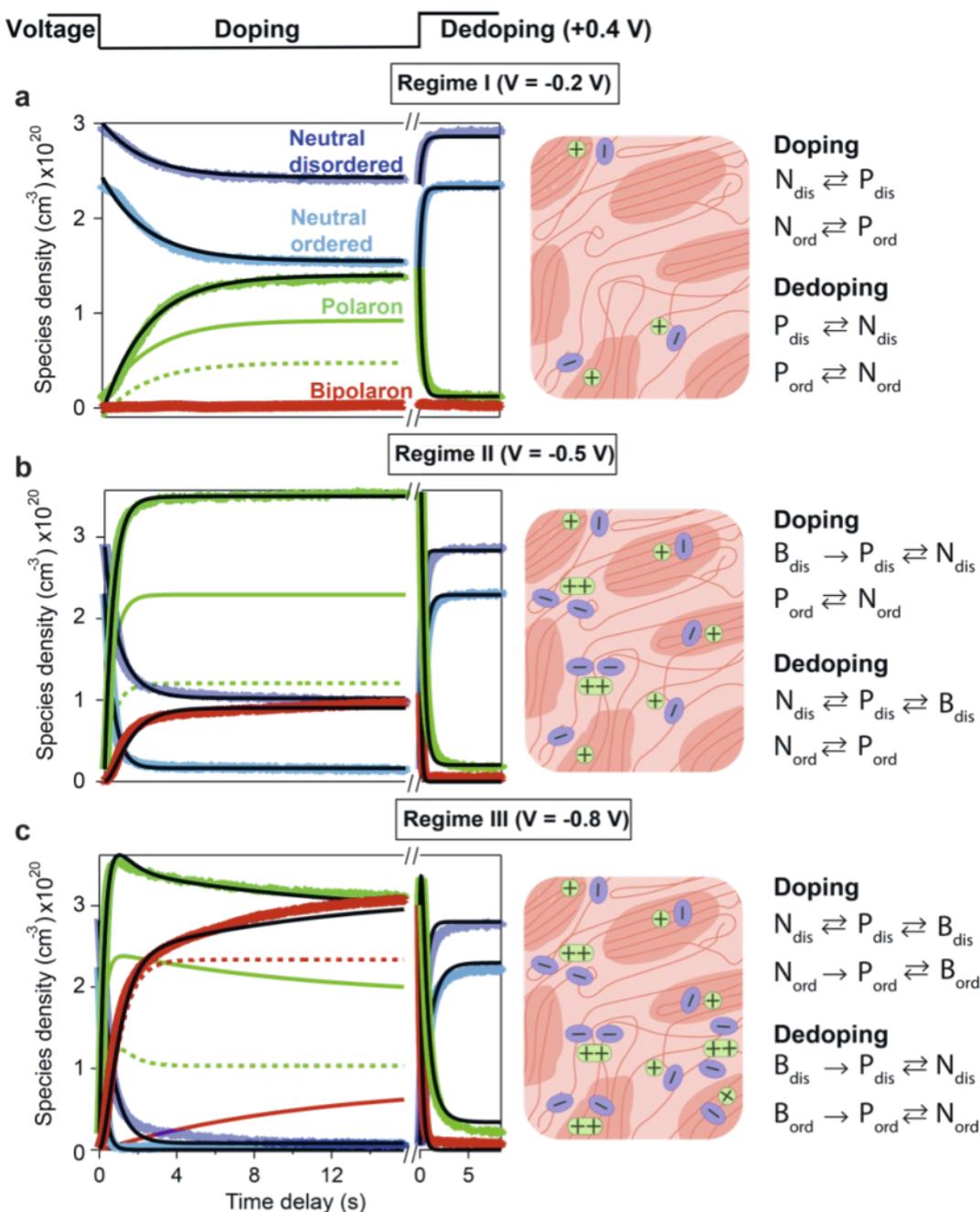
Fig. 2. Time-resolved concentrations of the neutral ordered and disordered, polaron and bipolaron during a doping and dedoping step in a) Regime **I** (V = -0.2 V), b) Regime **II** (V = -0.5 V), and c) Regime **III** (V = -0.8 V). In the illustration, the darker area represents the ordered domains, the purple symbol the anions and the green symbol polarons (+) and bipolarons (++).[6]

phological domains of the semicrystalline polymer film. The rate and equilibrium constants involved in the process are described elsewhere, and they are indicative of which processes are more favorable in each regime.[6]

In general, we observe that the doping mechanisms and kinetics are very distinct in the different morphological domains of the film, with bipolarons being more numerous in the disordered regions of the film. Polarons and bipolarons play different roles in conductivity,[12] and identifying how and in which domain they exist has a direct impact on improving conductivity and therefore OMIEC device performance.

3. Conclusion

In this work, we have shown how the combination of time-resolved Vis-NIR spectroelectrochemistry and spectral decomposition is a powerful tool for studying the fundamental aspects of OMIECs. Because the absorbance changes in conjugated polymers during doping are spectrally overlapping, an optimization method such as MCR is important to decompose the spectra and to gain knowledge on their evolution with voltage or time.

Conjugated polymer-based OMIECs are typically semicrystalline or amorphous. We show that ordered and disordered regions have very distinct doping mechanisms, with bipolarons being preferred in the disordered domains. This has a direct impact on electronic conductivity, and it is therefore important to take into account when designing novel materials for emerging electrochemical applications. The tools presented in this work are versatile and can be used to characterize any electrochromic material.

[1]   B. D. Paulsen, K. Tybrandt, E. Stavrinidou, J. Rivnay, *Nat. Mater.* **2020**, *19*, 13, https://doi.org/10.1038/s41563-019-0435-z.
[2]   H. F. P. Barbosa, G. D. G. Higuita, F. Günther, G. C. Faria, *Adv. Electron. Mater.* **2022**, *8*, 2100864, https://doi.org/10.1002/aelm.202100864.
[3]   P. Cavassin, A.-M. Pappa, C. Pitsalidis, H. F. P. Barbosa, R. Colucci, J. Saez, Y. Tuchman, A. Salleo, G. C. Faria, R. M. Owens, *Adv. Mater. Technol.* **2020**, *5*, 1900680, https://doi.org/10.1002/admt.201900680.
[4]   D. Marrero, A. Guimera, L. Maes, R. Villa, M. Alvarez, X. Illa, *Lab Chip* **2023**, *23*, 1825, https://doi.org/10.1039/D2LC01097F.
[5]   Q. Pei, G. Yu, C. Zhang, Y. Yang, A. J. Heeger, *Science* **1995**, *269*, 1086, https://doi.org/10.1126/science.269.5227.1086.
[6]   P. Cavassin, I. Holzer, D. Tsokkou, O. Bardagot, J. Réhault, N. Banerji, *Adv. Mater.* **2023**, *35*, 2300308, https://doi.org/10.1002/adma.202300308.
[7]   H. Shirakawa, *Angew. Chem. Int. Ed.* **2001**, *40*, 2574, https://doi.org/10.1002/1521-3773(20010716)40:14<2574::AID-ANIE2574>3.0.CO;2-N.
[8]   Z. Song, F. Chen, M. Martinez-Ibañez, W. Feng, M. Forsyth, Z. Zhou, M. Armand, H. Zhang, *Nat. Commun.* **2023**, *14*, 4884, https://doi.org/10.1038/s41467-023-40609-y.
[9]   R. Wu, M. Matta, B. D. Paulsen, J. Rivnay, *Chem. Rev.* **2022**, *122*, 4493, https://doi.org/10.1021/acs.chemrev.1c00597.
[10] C. Enengl, S. Enengl, S. Pluczyk, M. Havlicek, M. Lapkowski, H. Neugebauer, E. Ehrenfreund, *ChemPhysChem* **2016**, *17*, 3836, https://doi.org/10.1002/cphc.201600961.
[11] C. H. Camp, *J. Res. Natl. Inst. Stan.* **2019**, *124*, 124018, https://doi.org/10.6028/jres.124.018.
[12] D. Tsokkou, P. Cavassin, G. Rebetez, N. Banerji, *Mater. Horiz.* **2022**, *9*, 482, https://doi.org/10.1039/D1MH01343B.